Anthropogenic CO_2
Oceanic model
Diffusive-advective model
CO_2 absorption

CO_2 d'origine industrielle
Modèle océanique
Modèle diffusif-advectif
Absorption du CO_2

The absorption of fossil-fuel CO_2 by the ocean

F. MacIntyre
Graduate School of Oceanography, University of Rhode Island, Kingston, Rhode Island 02881, USA.

Received 1/10/79, in revised form 20/3/80, accepted 12/6/80.

ABSTRACT

All 74 ppm (1 ppm = 1.77 E 14 moles CO_2) of anthropogenic CO_2 can be accounted for in atmosphere (45 ppm) and ocean (29 ppm) by a simple "diffusive/descending-water" model. 3.8 ppm remain in the mixed layer (at equilibrium), 19.1 have diffused into intermediate waters (at 1.3 cm^2/sec), and 5.7 ppm have been advected by the North Atlantic Deep, and the Antarctic Intermediate and Bottom Waters. The diffusive uptake must be driven by a realistic "interrupted exponential" atmospheric driving function, with 23 years of no growth between the World Wars. The 575 m surface-ocean box required by a two-box air-sea equilibrium model, is a useful parameterization of diffusion plus thermohaline circulation, with only the 75 m wind-stirred layer near equilibrium. Future atmospheric projections from such a model are at the upper limit of those from kinetic box models, reaching 600 ppm by 2030 AD for most scenarios.

Oceanol. Acta, 1980, **3,** 4, 505-516.

RÉSUMÉ

L'absorption du CO_2 d'origine anthropogénique par les océans

Un modèle simple, fondé sur la diffusion et la descente des eaux océaniques vers le fond, permet de démontrer que sur l'ensemble des 74 ppm (1 ppm = 1,77 E 14 moles) de CO_2 ajoutés par l'activité humaine à l'atmosphère, 45 ppm se trouvent dans celle-ci et 29 ppm sont passés dans l'océan. Dans celui-ci, 3,8 ppm sont encore présents dans la couche supérieure qui est à l'équilibre avec l'atmosphère; 19,1 ppm ont diffusé dans les eaux intermédiaires (avec un coefficient de diffusion turbulente égal à 1,3 $cm^2.sec^{-1}$), et 5,7 ppm sont véhiculés de haut en bas par l'eau profonde Nord-Atlantique, ainsi que par les eaux Antarctiques intermédiaires et profondes. La fonction « absorption par diffusion » du CO_2 par l'océan introduite dans le modèle est « réaliste » car, tout en admettant l'accroissement exponentiel de la quantité de CO_2 dans l'atmosphère, elle tient compte de l'interruption de 23 ans qui correspond au non-accroissement de l'activité industrielle entre les deux guerres mondiales. Les 575 m pour la dimension verticale de la « boîte » océanique de surface requis par le modèle apparaissent significatifs, car ils rendent compte de l'influence à la fois de la diffusion et de la circulation thermohaline, sur la distribution du CO_2 anthropogénique dans l'océan. Dans cette boîte, seuls les premiers 75 m, qui correspondent à la couche mélangée par le vent, sont proches de l'équilibre avec l'atmosphère.
Les concentrations futures de CO_2 dans l'atmosphère que ce modèle permet de prévoir avoisinent les limites supérieures des valeurs prévues par les modèles cinétiques du type « boîtes », qui atteignent 600 ppm en l'an 2030, comme le prédisent la plupart des scénarios utilisés.

Oceanol. Acta, 1980, **3,** 4, 505-516.

ANTHROPOGENIC INPUT

Thanks largely to the work of Keeling (1973 *a*) and Rotty (1977), one of the better known portions of the CO_2 system is man's production from fossil-fuels and limestone. Figure 1 shows the exponential growth in CO_2 production over the last century. The most noteworthy feature of this growth is the severity of social dislocation required to force a departure from the exponential. Each of the three shaded abnormal periods corresponds to a historical trauma: World War I, which produced the longest-lasting effect on CO_2 production; the Great Depression, which caused the sharpest decrease; and World War II, which made barely a ripple. Together, these 11 abnormal years caused a 23-year delay in CO_2 growth, perhaps buying us time to anticipate and ameliorate whatever problems may lie ahead.

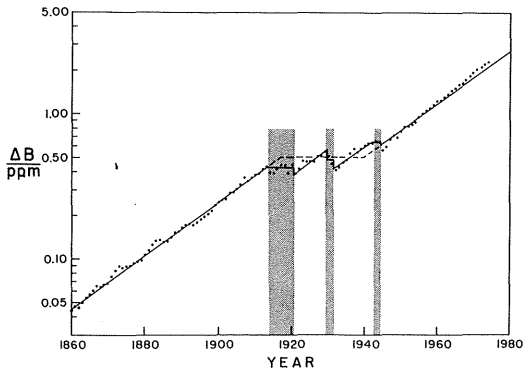

Figure 1

Annual production of CO_2 since the Industrial Revolution, after Keeling (1973 a). The 11 abnormal years (shaded) seem to have had little influence upon the 4.25 % annual growth rate, although they delayed production somewhat. The solid line is a piecewise log-linear approximation, while the dashed line is an even simpler estimate which holds production constant for the 23-year "stillstand" from 1917 to 1939, the "time of troubles" as recorded in the CO_2 data.

The unit "ppm" used in Figure 1 means "parts per million by volume", and is a mass unit equal to 1 μmole of CO_2 per mole of atmosphere – that is, 1.767 E 14 moles, 2.123 E 12 kg C, or 7.778 E 12 kg CO_2. The ppm is the natural unit for atmospheric concentrations, and its freedom from trailing exponents recommends it for easy discussion.

The solid line of Figure 1 is from an algorithm which reproduces the significant features of the historical curve. The dashed line is the even simpler version given in Table 1, which will be employed in the subsequent discussion. The horizontal portion of the dashed line will be called the "stillstand" – a 23-year interruption in an otherwise steady exponential.

The 4.25 % annual rate underestimates post-war growth, but the oil crises corrected this faster growth and returned production to the curve, as happened on several earlier occasions.

Eventually exhaustion of resources will depress this growth, leading to something approximating the logistic curve of Figure 2 (which is also generated by the algorithm of Table 1).

To hazard an interpretation of the 4.25 % growth rate, it might be partitioned into 2.1 % to keep pace with

Table 1

A pocket-calculator algorithm which generates the "interrupted exponential" CO_2-production curve of Figure 1 as the initial portion of the logistic curve of Figure 2. ΔB is the annual incremental production in year t, and B the corrected cumulative production to year t, while B′ is the uncorrected cumulation. The factor 1.018 corrects the calculated (mid-year) value of B′ to an end-of-year value to equal the summed ΔB's. ε corrects for accumulation during the stillstand. $\hat{B}$, the limiting value, is estimated from Armstrong (1974), and ajustable over the given range: other parameters are constrained by historical data (Keeling, 1973 a; Rotty, 1977; MacIntyre, 1978 a).

Exponential growth:	$dB/dt = aB$
Logistic growth:	$dB/dt = aB(1-B/\hat{B})$
$\Delta B = aB'(1-B'/\hat{B})$	$a = 0.0425$
$B' = \beta\hat{B}$	$\hat{B} = 1500 - 4100$
$B = 1.018\beta\hat{B} + \varepsilon$	$\Delta B_0 = \Delta B(1860) = 0.0455$
$\beta = [1 + e^{-at}(a\hat{B}/\Delta B_0 - 1)]^{-1}$	$a/\Delta B_0 = 0.9341$

year ≦ 1917	1917 ≦ year ≦ 1940	1940 < year
t = year-1860	$t = 56.0178$	t = year-1883
$\varepsilon = 0$	$\varepsilon = 0.4894$ (year-1917)	$\varepsilon = 11.256$

population growth, and 2.1 % to increase the standard of living in the West. Since mankind seems reluctant to reduce either of these numbers, the robustness of the 4.25 % growth rate over the past 120 years may indicate that it will take extraordinary social and economic pressure to depress the growth projected in Figure 2. Although pressures are increasing, the US is discussing 35 new coal-powered electric plants for the 1990's, and recent problems with fission power suggest that fossil-fuels will remain our most important energy source for some time. Conversion of coal to liquid fuel will increase the rate of CO_2 production, since fuel synthesis produces CO_2 during manufacture.

The upper curve in Figure 2 assumes complete consumption of the estimated 4 100 ppm of total reserves of fossil fuel (Armstrong, 1974). Although this value gives a better fit to the past, and has occasionally been used to make projections (Zimen, Altenheim, 1973), the 1 500-ppm curve, representing economically accessible reserves (Armstrong, 1974), seems more realistic. Much coal is in 30-cm seams, for which no extraction method now appears practical.

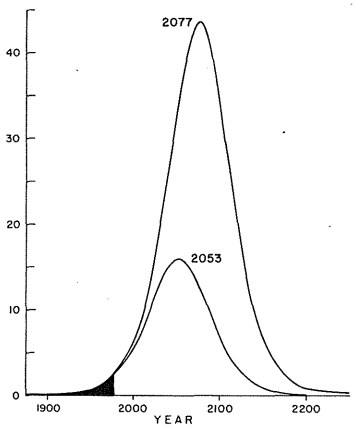

Figure 2

Annual CO_2 production in the future, from the algorithm of Table 1 as a function of fossil-fuel reserves. The 4 100 ppm "total reserves" curve puts an upper limit on possibilities, but the 1 500 ppm "economically accessible reserves" curve is more probable (Anderson, 1974). The year of maximum production is given for each curve, and the black area represents CO_2 already produced.

Although long-range projections may be of limited value, they do indicate that CO_2-related problems (whatever they may be) are unlikely to diminish in the future.

To summarize Figure 1, we have so far produced 75 ppm of CO_2. Some 46 ppm of this remain in the atmosphere, and it is our goal to determine how much of the "missing" 29 ppm may have gone into the ocean.

ON MODELS

The prospects of a CO_2-induced temperature rise have been well publicized (Arrhenius, 1896; Chamberlin, 1897-1899; Callendar, 1938; Plass, 1956; Tyndall, 1961; Broecker, 1975; Manabe, Wetherald, 1975; Augustsson, Ramanathan, 1977). Although there are many unknowns, a principal datum in assessing the probable threat is the partial pressure of CO_2 in the atmosphere at some future date. Many models (Bolin, Eriksson, 1959; Keeling, Bolin, 1967, 1968; Bacastow, Keeling, 1973; Oeschger *et al.*, 1975) have essayed projections, and although differing in detail, most agree that atmospheric CO_2 will double its pre-industrial value within the next 50 to 100 years. General-circulation atmospheric models suggest a consequent 2° rise in mean surface temperature (Schneider, 1975), although Newell, Dopplick (1979) and Idso (1980) find only 0.3°. Hoyt's (1979) deduction of a historical 0.4° warming from a 10 % CO_2 increase lends support to the larger figure.

The possible consequences of a 2° rise include a poleward shift of agricultural zones of some 50 km (extending the growing range North, but also extending the range of pests, and detuning the fine match between environment and cultivar), an increase in weather instability at the critical ends of the growing season, and melting of the West Antarctic ice sheet (which is grounded below sea level), resulting in a 5 m rise in sea level (Mercer, 1978; Thomas *et al.*, 1979; Colville, 1977). Since the Sahelian drought was caused by a similar shift in rainfall patterns, droughts in other semi-arid, but more populous, regions (e. g. Anatolia to the Deccan, Mexico, the Hwang Ho basin, etc.) might be anticipated.

Because the lead time for any technological fix or societal response to such problems is more likely to be decades than years, the two-fold uncertainty of the corpus of models is larger than one would like, and one must find ways to choose among them. But in that case, why create yet another model?

There are several reasons. First, a different point of view may be the most direct way to examine other approaches. Second, one may wish to examine the effect of small changes in parameters or assumptions: in practice this is impossible without access to the original program and computer. Third, a point often overlooked – social change of the magnitude needed to reverse the world's energy policy is likely to come only with wide-spread perception of the threat. As I see it, this means that the models (from which the threat is necessarily derived), must be understandable and believable to the staff of the average politician. A megacomputer model accessible only to its creator may not be the best instrument on which to play a clarion call for action.

All three of these needs are addressed by the development of pocket calculators smart enough to cope with world-CO_2 models. Manifestly, these data-poor machines require a fresh approach, but the resulting models are conceptually simple, and anyone, anywhere, can change a parameter and see what happens. An additional benefit is the 30-fold reduction in computer costs. For peer acceptance, simple portable models should reproduce the projections of megamodels which have received general approval (e. g. Bacastow, Keeling, 1973; Oeschger *et al.*, 1975).

The first pocket model began from the obvious: air and sea are in approximate mean global equilibrium, despite local factor-of-two departures, and despite man's perturbation of the steady state. The resulting framework – the so-called "minimal model", or MM (MacIntyre, 1978 *a*) – duplicates the historical data, and Bacastow and Keeling's (1973) projections with remarkable fidelity, at the cost of demanding a surface ocean in equilibrium with the atmosphere which is 575 m deep.

This depth is a fitting parameter, and, like the "residence times" of kinetic box models, is not to be taken too seriously. Nydal (1968) and Suess (1970) noted a 25-fold variation in atmospheric residence times among CO_2 models; the surface-ocean residence time (with respect to transfer to deep water) varies by a similar factor (Craig, 1957; Gulliksen *et al.*, 1972; Rafter, O'Brien, 1972). This range cannot be attributed to a difference between $^{12}CO_2$ and $^{14}CO_2$, for as Oeschger *et al.* (1975) point out, the exchange coefficient between the mixed layer and the deep sea is 10-fold greater for bomb-produced $^{14}CO_2$ than it is for natural $^{14}CO_2$. They also note a three-fold increase for fossil $^{12}CO_2$ above natural $^{14}CO_2$, and suggest that the difference in exchange coefficients arises from differences in the production functions for the three varieties of CO_2. Upper-atmosphere ^{14}C is produced steadily, at a uniform rate; bomb ^{14}C is created in pulses; and fossil-fuel ^{12}C is released exponentially. Table 3 indicates the variation in diffusive uptake that follows from these three time-dependent boundary conditions, and it is not surprising that a model which does not take this behavior into account will find that its adjustable "constants" must be rather flexible.

An equilibrium model must also compensate for extraneous events, and it does so by creating an excessively deep surface box to replace diffusion and thermohaline circulation. In both cases, the justification for arbitrary parameterization is pragmatic: if it works, it may be useful; when it fails, it may point to the needed refinement. In the present case, the 575 m surface box cries for explanation.

A THERMODYNAMIC DIVERSION

Although not strictly necessary for a discussion of the past, the most important parameter for the future of the world CO_2 system is the relation between changes in the partial pressure of CO_2 in the atmosphere, P, and consequent changes in C, the total dissolved CO_2 in seawater, all measured at constant total alkalinity

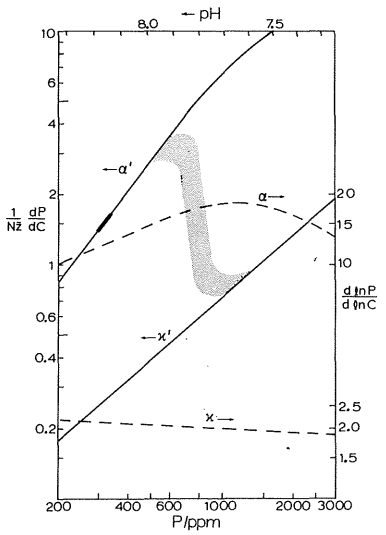

Figure 3:

The effective partition function measures the distribution of an increment of CO_2 produced in terms of (ppm-to-air)/(ppm-to-sea), and the increase with P indicates that between now and 2030 AD the fraction of anthropogenic CO_2 remaining in the atmosphere will increase sharply. The heavy segment on α′ represents the historical change over the last 120 years. The transition between α′ and ϰ′ occurs as carbonates begin to dissolve, but is illustrative only, since many non-thermodynamic effects enter into this transition. On the right-hand scale, $\alpha = d \ln P / d \ln C$ approximates the "Revelle factor" or "buffer factor", and ϰ is its constant-carbonate value. For P < 620 ppm, and for an ocean at 5°C, 35°/₀₀ salinity, and 2.3 eq/m³ total alkalinity, $\alpha' = (6.510\,E\text{-}4)\,P^{1.348}$. The symbols memorialize Buch's (1930) recognition of the importance of such functions and the name he chose for dC/dP, "Aufnähmekapazität", with α for constant alkalinity and ϰ for constant carbonate. N is (m²/ocean) × (ppm/mole), c.2, and ẑ the depth of the CO_2-absorbing box at 575 m.

("constant alkalinity" is the oceanographer's version of proton conservation. Ignoring small natural changes in minor protolytes such as NH_3, PO_4^{3-}, H_2S, etc., only the precipitation or dissolution of carbonate sediments will alter the alkalinity in a CO_2 model).

For the sake of mnemonics (air above, C below), we work with the coefficient $(\partial P / \partial C)_A$. Kurt Buch (1930, p. 78) called this the "Abgabefähigkeit", or "delivery capacity". Revelle and Suess (1957) renamed a quasi-logarithmic version of this the "buffer factor" (not to be confused with van Slyke's "buffer value" $dC/d\text{pH}$ [1922]). Traditionally (Revelle, Suess, 1957; Machta, 1972; Fairhall, 1973), this coefficient has been thought of as a constant, near 10. Keeling (1973 *b*) was evidently the first to use a time-dependent "buffer factor".

I will call this object a "partition function", for it depends upon temperature, salinity, and most importantly, upon pH and thence upon the amount of CO_2 already absorbed by the surface ocean. Figure 3 shows the range of values taken by four related functions plotted against P. Although it has been possible to ignore the variation of partition functions in the past, it must be taken into account in the future.

The algebra behind Figure 3 is tedious but not difficult (MacIntyre, 1978 *a*, 1980) and follows directly from the chemical reaction coefficients (equilibrium "constants") of H_2CO_3, which are themselves functions of temperature, salinity, and pressure in seawater. Approximate values are given in Table 2.

The functions on the left of Figure 3 are dimensionless "effective" coefficients having the significance "ppm-to-air/ppm-to-sea", giving an immediate indication of how CO_2 added to the atmosphere is ultimately partioned between air and sea. They are obtained by dividing the purely thermodynamic quantity $(\partial P / \partial C)$ (which has dimensions $\text{ppm}/(\text{M}/\text{m}^3)$ by (3.6 E 14m^2/ocean).(ppm/1.8 E 14 M).[depth of equilibrium-surface ocean]). This depth is not known *a priori*, and is the 575 m depth of MM. There appears to be a tendency to assume that the historical value of α′ is near 1, but this is not in agreement with such data as we have (see MacIntyre, 1978 *a*, for a description of the data fitting). We are currently on the curve labelled α′, which is the effective partition function at constant alkalinity, and will remain on this curve until the ocean becomes sufficiently acidic (by absorbing CO_2) to dissolve high-magnesian calcite sediments in shallow waters. The timing is difficult to predict, because there is no single thermodynamic value of calcite solubility in the ocean. But somewhere between pH 7.9 and 7.7, this transition will occur, and the neutralization of anthropogenic CO_2 will be taken over by carbonate dissolution in surface waters. This greatly increases the capacity of the ocean to absorb CO_2, and drops the effective partition function to the lined labelled ϰ′, from c.3 to somewhat below 1. The immediate consequence is that atmospheric accumulation slows down dramatically. Unfortunately, this drop may come later than one might wish.

Many writers (see Anderson and Malahoff (1978) for a variety of approaches) consider that the c.3-fold supersaturation of surface waters requires that carbonate dissolution be limited to deep waters, apparently thinking in terms of the millenial time-scale of abyssal circulation for the change from α to ϰ. On the contrary, the high carbonate-ion concentration is itself a useful sink for atmospheric CO_2. Further, shallow-water carbonates show etch pits under the electron microscope, indicating at least seasonal dissolution in carbonate-saturated waters (Alexandersson, 1975) and suggesting

Table 2

The principal chemical reactions of carbonic acid and the associated thermodynamic reaction functions (equilibrium "constants"). All of the Ks are functions of temperature, pressure, and salinity in the ocean (Millero, 1979). Most "CO_2" in the atmosphere-ocean system is actually in the form of bicarbonate.

$CO_2\,(\text{gas}) \rightleftharpoons CO_2\,(\text{aq})$ $CO_2\,(\text{aq}) + H_2O \rightleftharpoons H_2CO_3$	$K_0 = P(CO_2)/[H_2CO_3 + CO_2\,(\text{aq})] \simeq 10^{-5}$
$H_2CO_3 \rightleftharpoons H^+ + HCO_3^-$	$K_1 = \{H^+\}[HCO_3]/[H_2CO_3 + CO_2\,(\text{aq})] \simeq 10^{-7}$
$HCO_3^- \rightleftharpoons H^+ + CO_3^{2-}$	$K_2 = \{H^+\}[CO_3^{2-}]/[HCO_3^-] \simeq 10^{-10}$
$CaCO_3 \rightleftharpoons Ca^{2+} + CO_3^{2-}$	$K_{sp} = [Ca^{2+}][CO_3^{2-}] \simeq 10^{-6}$
$B(OH)_3 \rightleftharpoons H^+ + H_2BO_3^-$	$K_B = \{H^+\}[H_2BO_3^-]/[B(OH)_3] \simeq 10^{-9}$

that shallow-water carbonates respond rapidly to atmospheric CO_2. The rate of attack is a function of departure from equilibrium and impossible to predict with any confidence at this time. But I would not recommend that any seaport build a limestone quay.

Gas exchange velocities across the sea surface are near 30 μm/sec in both field (W. S. Broecker, Peng, 1974) and laboratory (H. C. Broecker, 1979). At atmospheric CO_2 concentrations this is 25 ppm/year (12.4 moles/m^2.year), or ten times the current CO_2 production, indicating that interphase transfer is not a rate-limiting step in the uptake of CO_2 by the ocean.

MODELING THE CARBOCLINE

Contributing to the difficulty of assessing air-sea CO_2 differences is the sharp gradient of total dissolved CO_2 in seawater. Nearly every oceanic profile shows a biologically produced CO_2 decrease at the surface, and a mid-water maximum at 1-1.5 km. The gradient near the surface – the "carbocline" – is a dynamic phenomenon created by eddy diffusion, advection, production and consumption by organisms, and absorption from the atmosphere. Evaluating the contributions of these mechanisms is an important but complex problem. Simplification begins by neglecting major horizontal motions and considering a one-dimensional vertical model. Fortunately, horizontal advection is important only when CO_2 varies laterally, and areas can be found where the vertical model will work. Small horizontal motions – and in particular the sinking of surface water along isopycnals that intersect the sea surface – are incorporated into a high vertical eddy diffusivity. Although the diffusivity so defined is an omnibus parameter which cannot be directly measured, and which is probably an order of magnitude higher than the true vertical turbulent diffusivity, its value is nonetheless sharply constrained by observed gradients in the ocean.

In the following discussion, the $z=0$ level is not the sea surface, but the bottom of the nutrient-depleted layer (which is often a bit deeper than the mixed layer of uniform temperature and salinity).

The differential equation of the vertical production-advection-diffusion model will be taken as

$$\partial C/\partial t = D(\partial^2 C/\partial z^2) + w(\partial C/\partial z) + J e^{-\mu z}, \qquad (1)$$

where D (m^2/year) is the diffusivity, w (m/year) the vertical advection velocity, and J (M/m^3.year) the CO_2 production rate at the surface. Since solutions are known only for $\partial C/\partial t = 0$ and constant w, previous models (Wyrtki, 1962; Munk, 1966; Craig, 1969; Craig, Weiss, 1970) have avoided the carbocline and placed an arbitrary upper boundary a kilometre from the surface, at a depth where w can reasonably be assumed constant. Full-scale numerical solution of (1) is no doubt possible, but some progress can be made by further simplification. First, we examine the steady-state condition ($\partial C/\partial t = 0$) with varying w.f. This requires solution of the steady-state difference analog of (1):

$$C_i = \frac{1}{2}\{(C_+ + C_-) + [w_i(C_+ - C_-)/2 + \delta J_i]\delta/D\}, \qquad (2)$$

where C_i, C_+, and C_- are the concentrations at the i-th depth step, the step above, and the step below, respectively, and δ is the depth-step size.

None of the coefficients is well known. The best available estimate of CO_2 production comes from the oxygen-consumption estimates of Riley (1951, North Atlantic) and Packard (1971, Eastern tropical Pacific). Based on this work, we will adopt

$$J e^{-\mu z} = 0.016\, e^{-0.0035z}\ \mathrm{M/m^3.year}.$$

The simplest plausible function for $w(z)$ is harmonic

$$w(z) = w_b \sin(\pi z/2z_b),$$

where w_b is a constant speed, vertical at the arbitrary lower boundary z_b (here taken as 2250 m), horizontal at the surface, and directed along a circular arc through the carbocline. With this motion, continuity is preserved, and no violence is done to one-dimensionality as long as the CO_2 concentration is uniform over horizontal regions of width z_b (or, for our 120 year period of interest with $w_b = 3.5$ m/year, 420 m).

This leaves the diffusivity. In deep water (1 to 4 km), the usual estimates are 1-2 cm^2/sec (Munk, 1966; Craig, 1969), with w being 1-5 m/year. Extracting better values is an exercise in curve fitting, as exemplified by Figure 4.

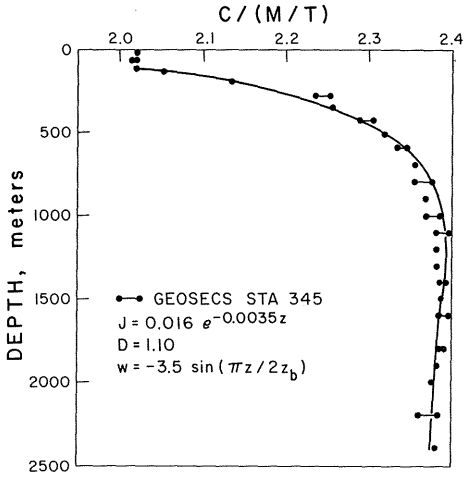

Figure 4:
The vertical production-advection-diffusion model of total dissolved CO_2, assuming steady state. Only certain ocean regions are sufficiently free of large-scale horizontal motions for this model to be realistic. The data here are from the Eastern tropical Pacific (Geosecs Station 345). Where 2 values are given for a single depth, they represent analyses by different techniques. The solid line is a numerical solution to the model with a variable advection velocity as given in the Figure.

The consistent result is that D = 1.3 cm^2/sec is a reasonable value, as Oeschger *et al.* (1975) found by a different approach (D = 1.26 cm^2/sec).

The upward CO_2 flux at the surface is

$$\varphi = -D(\partial C/\partial z)_{z=0},$$

which for Figure 4 is $-4100\ (0.00099) = -4.06$ M/m^2.year, or 8.3 ppm/ocean-year. The utility of this number is that it must be equal to the amount of carbon carried down annually by mechanisms which are less easy

to quantify. The principal downward transporting agent is probably "Ketchum's yoyo" (Ketchum, 1957; Munk, 1966; MacIntyre, 1978 *a*), the daily vertical migration of the "deep-scattering-layer" organisms, which ascend toward the surface at sunset to consume the day's crop of phytoplankton (and each other) and descend again at sunrise to respire 60 % of the ingested carbon (Menzel, 1974) at daytime resting depths as deep as 1 200 m. Gravitational settling of detritus and fecal pellets, which lose half of their mass to bacterial oxidation within the first 500 m, are another important downward pathway (Johannes, Satori, 1966; Vinogradov, 1961).

In the usual units of biological productivity, 8.3 ppm/ocean-year is 48.7 gC/m^2-year, close to the traditional open-ocean estimate of 50 gC/m^2-year.

Anticipating one of the following chapters (see "the diffusive subsurface in greater detail"), we note that as CO_2 increases in the atmosphere, the surface gradient must become smaller. The downward flux is constant, because it is biologically mediated and controlled by the rate at which the limiting nutrient (phosphate) is recycled to the surface by upwelling. Thus the annual uptake by the ocean must just equal the difference between the constant downward flux and the reduced flux returning along the lessened gradient.

A POCKET-CALCULATOR DIFFUSIVE MODEL

The parameters of an ideal model should be directly measurable quantities. But as noted above for diffusivity, the need to average out turbulence and intermittency makes measurements difficult. By approaching from the other direction, integrating in space over the world ocean and in time over the last 120 years, one may find realistic parameters which offer a simple picture of how the system has behaved thus far.

The thermodynamic constraint on a time-integrated equilibrium model is that initial and final states have equal CO_2 partial pressures in surface ocean and atmosphere. MM's global ocean has a temperature of 5°C, a salinity of 35°/$_{oo}$, and a total alkalinity of 2.3 eq/m^3: by straightforward calculation, the total-CO_2 concentrations in equilibrium with the initial (292.5 ppm) and final (337.3) atmosphere are 2.093 and 2.118 M/m^3 (such precise constraints on ocean composition are not a normal feature of kinetic box models, which have been known to absorb CO_2 so wantonly (MacIntyre, 1978 *a*) that their oceans have partial pressures far in excess of their atmospheres, by trusting to mass balances without thermodynamic checks).

The 5° temperature, although an effective mean value, and somewhat arbitrary, is not a free parameter. That it is well below the area-weighted average, *c* 20°, indicates that warm waters (regions of CO_2 evasion) do not control the system. This is more than a datum or hypothesis: it is an absolute thermodynamic constraint. The complex kinetics that must occur to make this happen are of considerable interest, and include tropospheric, surface ocean, and thermohaline circulation patterns. Also important are the distribution of wind stress on the ocean and its correlation with temperature, and perhaps smaller-scale phenomena involving the physicochemical hydrodynamics of the sea. However these factors blend together, the result is that CO_2 evasion from warm waters is less important in setting the atmospheric level than CO_2 uptake by cold waters.

It is reassuring to those who distrust equilibrium models of such complex kinetic situations, to find that the absolute equilibrium employed in this model may be replaced by a constant departure from equilibrium. Imposing an arbitrary disequilibrium of 10 ppm (somewhat larger than the noise level of estimates of mean surface-ocean P_{CO_2}) does not appreciably alter the properties or conclusions of an equilibrium model, and displaces its time predictions by only a few years.

The small change in total CO_2 (0.025 M/m^3) generates the 575 m surface box of MM, for this is the volume required to hold the 29 ppm (14.12 M/m^2) that have disappeared from the atmosphere. This depth must be reached on an annual, global basis, under the constraints of the model. Mixing to 75 m occurs nearly universally, and to perhaps a kilometer in the winter waters of the Norwegian and Bellingshausen Seas. But on a global basis, there is no physical expression of a 575 m box.

The other extreme among simple models is a purely diffusive ocean. Assuming an effective vertical diffusivity D sufficiently large to maintain the system at steady state, the 575 m rectangular box (in concentration-depth coordinates) becomes an 1 150 m deep triangle.

Between the end members of a purely equilibrium ocean and a purely diffusive ocean, lies a continuum of equilibrium-surface / diffusive-subsurface models. Despite the presence of two boxes, these are not two-parameter models, since (if constrained to accept 29 ppm under any simple atmospheric-growth law) the depth of the surface box *z* and the diffusivity must lie along a parabolic curve in *z*-D coordinates. Unfortunately, no point on such a curve passes through truly acceptable values of both parameters. Either *z*, or D, or both, is larger than is physically plausible.

THE DIFFUSIVE SUBSURFACE IN GREATER DETAIL

Because the diffusion equation is quite sensitive to the surface boundary condition, the next step is to refine the atmospheric forcing function P(*t*), to give an analytic approximation that bears some semblance to reality.

Let us take the interrupted exponential of Figure 1 as adequately representing the CO_2 production function, and assume that over the historical period, the air/sea partition function α' has remained constant. This leads immediately to a three-piece P(*t*) as shown in the upper curve of Figure 5. The stillstand (Region II) now appears as a slight flattening of the curve in the middle years.

Reliable measurements of P are very recent, and the longest series is from the Mauna Loa Observatory

Table 3

Diffusion into a semi-infinite region with zero initial concentration, for three simple surface-boundary conditions. The notation "i^2 erfc x" signifies the second integral of the complementary error function, and $x = z/2\sqrt{D\,t}$. The equations are optimized for curve segments starting at (C_0, 0) and increasing by C_s and T in concentration and time. These solutions are to be added to the VAPD solution of Figure 5. Note the relationship $C = C_0 + C_2(e^{kt} - 1) = C' + C_2 e^{kt}$ with $C' = C_0 - C_2$.

Growth Law	Concentration	Total Absorption	Annual Flux
$C(0, 0) = 0$	$C(z, 0) = 0$	$Q(t) = \int_0^\infty C(z, t)\,dz$	$\varphi(t) = dQ/dt$
		$= \int_0^\infty \varphi(t)\,dt$	$= -D(\partial C/\partial z)_{z=0}$
$C(0, t) =$	$C(z, t) =$		
Step:			
C_s	C_s erfc x	$2C_s\sqrt{D\,t/\pi}$	$C_s\sqrt{D/\pi t}$
Linear:			
$C_1 t$			
$C_1 + C_s/T$	$4C_1$ ti^2 erfc x	$(4/3)C_1 t\sqrt{D\,t/\pi}$	$2C_1\sqrt{D\,t/\pi}$
Exponential:			
$C_2(e^{kt} - 1)$			
$C_2 = C_s/(e^{kT} - 1)$	$\frac{1}{2}C_2 e^{kt}[e^{z\sqrt{k/D}}\,\text{erfc}\,(x + \sqrt{kt})$	$C_2[e^{kt}\sqrt{D/k}\,\text{erf}\,\sqrt{kt} - 2\sqrt{D\,t/\pi}]$	$C_2 e^{kt}\sqrt{kD}\,\text{erf}\,\sqrt{kt}$
	$+ e^{-z\sqrt{k/D}}\,\text{erfc}\,(x - \sqrt{kt})] - C_2\,\text{erfc}\,x$		

(Keeling *et al.*, 1976). These are shown dotted as annual means from 1959 to 1971. The perturbations on the MLO data have been related to surface temperature anomalies (MacIntyre, 1978*b*) and to the Southern Oscillation (Bacastow, 1976).

Concomittant with the atmospheric increase is the equilibrium rise in C shown as the bottom curve in Figure 5. As noted earlier, it is difficult to detect so small a change in the upper ocean. However, if we accept this version of $C(t)$ as the upper boundary condition for diffusion into a semi-infinite slab, the equations of Table 3 let us calculate how much CO_2 has been absorbed by the ocean. Table 4 sets out the numerical values of $C(t)$ at the ends of each segment. The values of C follow directly from the given values of $P(t)$ via the standard thermodynamic equations of Table 2. In

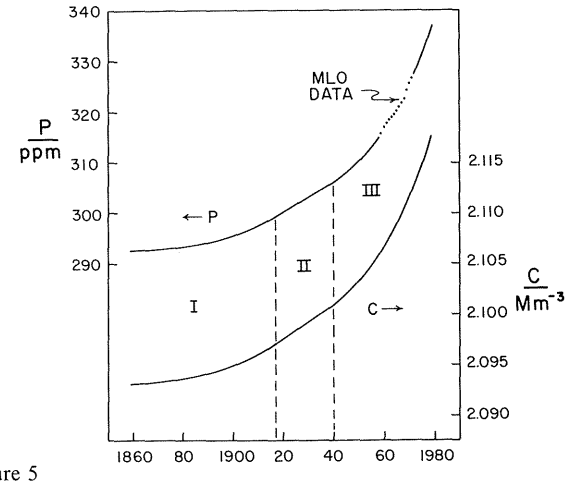

Figure 5

The interrupted-exponential production curve leads to these curves for atmospheric partial pressure P *and total dissolved* CO_2 *in the wind-stirred layer. The stillstand in region II appears as a linear increase, while regions I and III retain their exponential character. The data points are from the* 13*-year record of the Mauna Loa Observatory* (*Keeling* et al., 1976). *Piecewise approximations for* C *are*

$C_I = 2.092\,616 + (3.86\,E\text{-}4)\,[\exp 0.042\,094\,(year\text{-}1859)]$

$C_{II} = 2.097\,051 + (1.716\,E\text{-}4)\,(year\text{-}1917)$,

and

$C_{III} = 2.096\,554 + (4.44\,E\text{-}3)\exp[0.039\,8\,(year\text{-}1940)]$.

The greatest error occurs around 1960, *when the exponential approximation lies* 0.000 1 *below the equilibrium value.*

Table 4

Sample calculation of diffusive absorption of CO_2 *over the last* 120 *years, under the assumptions of Table* 5. *See text for* Q_{II} *and* Q_{III} *with non-zero boundary condition* (*the calculations may be good to* 3 *figures, but those who wish to replicate them will appreciate the additional digits retained in pH*, C *and k*).

Year	1859	1917	1940	1979
pH	8.188 117	8.179 439	8.170 888	8.134 067
B/ppm	1.045	12.24	23.51	74.75
P/ppm	292.46	299.27	306.12	337.27
C/(M/m^3)	2.093 002	2.097 051	2.100 998	2.117 538

Period	I	II	III
T/year	58	23	39
k/year^{-1}	0.042 094	1.716 1 E-4	0.039 800
Q/ppm	2.320	2.101	8.601
φ_T/ppm	0.116	0.122	0.506

estimating ΔC I have assumed $\Delta C = \Delta B - \Delta P$, or that there are no other CO_2 sinks which are not balanced by such sources as we have ignored.

The price paid for the analytic solutions of Table 3 is that we have ignored vertical advection. However, with w going to zero at the surface where absorption is maximal, and the small relative change, we may hope that the error introduced by this approximation is small. One cannot get the total absorption by piecewise integration using the functions of Table 3, since after period I the initial value is no longer zero. Rather than resorting to full-scale numerical integration (cf. Oeschger *et al.*, 1975), we pursue a more direct approach. There are several alternatives, all of which yield a total absorption within 1 ppm. Figure 6 will help explain the approach used here.

First, the exponential-growth concentration profile at the end of period I is the curve at the left of Figure 6. Q_I is 2.320 ppm for this profile. Next, we duplicate this Q_I with a *linear*-growth law which has the same slope as period II's. To do this, we must move the initial point in both time and concentration, solving

$$\left.\begin{aligned} C_s/T &= 1.716\ \text{E-4}, \\ C_s T^{1/2} &= (3Q/4)(\pi/D)^{1/2}/2.054 = 0.023\,546, \end{aligned}\right\} \quad (3)$$

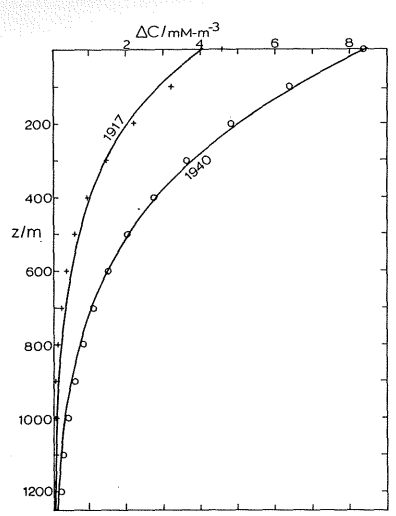

Figure 6

Coincidence of diffusion profiles. The approximate agreement of the 1917 *pairs (on the left) and of the* 1940 *pairs (right) make possible the replacement of the piecewise boundary condition of Figure* 5 *by a single exponential over a different time period. The solid line at the left is the incremental addition produced by the exponential growth of period I given in Table* 4. *The crosses approximating this profile are from the linear replacement given by equation* (3). *This same growth law continued to* 1940 *creates the solid line at the right, and is in turn approximated by the circles, representing an* 81*-year exponential growth from* 2.109 161 *to* 2.117 538 M/m^3. *In each case the total uptake* Q *is matched, and the approximation consists in striving for the best match of profiles.*

for C_s and T (the first equation is the known slope of period II; the second, a rearrangement of the linear equation for Q. The numerical factor is $(m^2/\text{ocean}) \times (\text{ppm/mole})$). The results are T = 26.60 year and $C_s = 0.004\,565$, so that C = 2.092 486 + (4.565 E-3) (year − 1 890.4). This substitution enables us to combine periods I and II into a single integration, with a zero initial boundary.

Table 5

The major assumptions behind the diffusive model. A capsule justification for each assumption is listed parenthically.

1. Only fossil-fuel CO_2 production, and an oceanic sink, are considered.
   (1) The diffusion equation is linear. Other putative anthropogenic sources are absorbed independently or balanced by comparable sinks.
2. CO_2 production follows a 4.25 %/year logistic curve from 1859 to 1979, except for a 23-year stillstand from 1917 to 1940.
   (2) The 2nd-order perturbations of Figure 1 are ignored.
3. Atmospheric retention has been constant at 60.8 %.
   (3) The change in α′, the pH-dependent equilibrium air/sea partition function, during this period was from 1.371 to 1.666, corresponding to an atmospheric retention increase from 57.8 to 62.5 %.
4. The 1958-1972 atmospheric mean coincides with the observed Mauna-Loa mean for the same period.
   (4) The mean is adjusted by setting the pre-industrial value of P to 291.82, the value it would have had if fossil-fuel were the only important input.
5. The ocean (at 5°C, 35°/$_{oo}$ salinity) is in mean global CO_2 equilibrium with the atmosphere, or departs from equilibrium by *c.* ±10 ppm over the 120-year period.
   (5) This constraint in the equilibrium model MM yields historical and future estimates which are essentially indistinguishable from those of Bacastow and Keeling (1973).
6. The CO_2 content of the mixed layer of the ocean increases exponentially (or linearly) along with the atmosphere.
   (6) This ignores 2nd-order non-linearities in the thermodynamic equations.
7. The effective mean global vertical eddy diffusivity D is 1.3 cm^2/sec.
   (7) D may be adjusted at will, with diffusive uptake varying as $D^{1/2}$. However, a factor of two in either direction produces severe deformations of observed gradients in the ocean.

The resulting 1917 (period I) profile is shown by the crosses at the left of Figure 6. Accepting the mismatch between profiles, we continue this linear growth through period II, to arrive at the solid line at the right of Figure 6, for which $Q_{I+II} = 5.908$.

Now we replace the period-(I + II) linear law by a period-(I + II + III) exponential, matching Q_{I+II}. Equations corresponding to (3) are transcendental for exponential growth, but trial shows that Q_{I+II} can be matched by

C = 2.091 432 + (9.566 E-3) exp [0.025 742 (year-1940)],

which passes through the end points of period III (and is only 0.0009 above the 1960 equilibrium value of C). From this curve, $Q_{I+II+III} = 19.11$ ppm. The 1940 (period-II) profile for exponential growth is shown by the circles at the right of Figure 6.

We have accounted for 2/3 of the "missing" CO_2 in this manner. The assumptions behind this calculation are important enough to merit separate display, and are gathered together in Table 5, which also shows a capsule justification for each assumption.

DESCENDING WATERS

The slow upward advection of water through the carbocline nearly everywhere is balanced by an equal volume of downward-flowing water in localized areas. We now investigate the transport of CO_2 by this component of the thermohaline circulation. The three principal water masses involved are the North Atlantic Deep (NAD, including Labrador Sea Water), the Antarctic Intermediate (AAI), and the Antarctic Bottom (AAB). The production rates of these three are, respectively, 15, 43, and 17 sverdrups (1 sv = 10^6 m^3/sec) (Gordon, 1971), and all three are formed at, or very near, the surface. Over the years they may have transported appreciable quantities of CO_2 from the atmosphere directly to abyssal waters. The North Pacific Intermediate Water, although possibly important, will be left for the future, as its production rate is inadequately known (Reid, 1973), and we ignore the small-volume warm waters like Red Sea and Mediterranean.

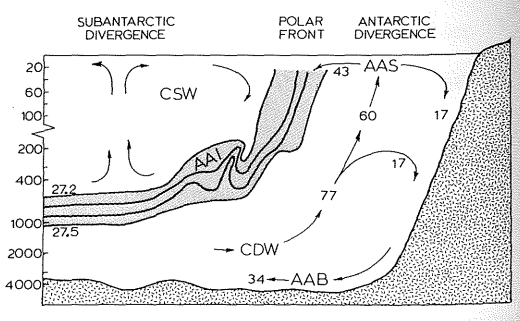

Figure 7

Antarctic circulation between New Zealand and the Ross Sea (taken as typical of the Southern Ocean). The several water masses (each distinguished by a more or less sharply defined area on a temperature salinity diagram) are: AAB = Antarctic Bottom; AAI = Antarctic Intermediate; AAS = Antarctic Surface; CDW = Circumpolar Deep Water; CSW = Circumpolar Surface Water. The annual transport at various locations is given in sverdrups. The surfaces of constant density at 1.027 2 *and* 1.027 5 T/m^3, *which delimit the descending AAI, are traced from Houtman* (1967). *AAB trickles down the edge of the continent to ventilate the sea floor with its high oxygen content. Note that the depth scale changes from linear to logarithmic at* 150 *m.*

Table 6

Thermodynamic parameters for the descending water masses. Curious as it may seem, the reaction functions are so poorly known (MacIntyre, 1978 b; after Lyman, 1957, and Weiss, 1974) that each investigator has tended to generate his own algorithms from the various determinations available. As a result, no two computations are identical, and to avoid confusion it is necessary to make clear what values are being used. Although absolute concentrations computed by various K_i-sets may differ appreciably, concentration differences, with which we are concerned, are fairly consistent. B_t is total boron and K_B the ionization function for boric acid.

	Water Mass		
	NAD	AAI	AAB
t/°C	4.00	1.50	−0.50
S/°/$_{oo}$	35.00	33.90	34.66
A/(eq/m^3)	2.380	2.302	2.354
B_t/(M/m^3)	0.4201	0.4068	0.4159
K_0/E-5	5.406	5.973	6.425
K_1/E-7	8.199	7.911	7.835
K_2/E-10	4.270	3.828	3.667
K_B/E-9	1.362	1.274	1.246

NAD appears to be formed by winter cooling south of Greenland and also in the Norwegian Sea, where it forms a relatively homogeneous layer several hundred meters deep which spills over the Greenland-Iceland Rise. Events in the Southern Ocean are more complex, and Figure 7 attempts to generalize the circulation pattern. The source water for both AAI and AAB is the Circumpolar Deep Water (CDW). Since it has been several hundred years since CDW could exchange heat, water, and CO_2 with the atmosphere, its properties have not changed during the Industrial Revolution. CDW rises to the surface by displacement, forced up by descending waters, and upon reaching the surface at the Antarctic Divergence to become Antarctic Surface Water (AAS), it takes two disparate routes. A south-flowing moiety is cooled and picks up salt rejected by winter freezing of shelf ice. Both events make it heavier, and finally it sinks as the initial constituent of AAB. The north-flowing portion is warmed and diluted by fresher water from summer melting of ice, becoming lighter by both processes. Nevertheless, it is still heavier than the Circumpolar Surface Water (CSW), and so plunges down at the Polar Front to become AAI.

In dealing with specific water masses, it seems appropriate to use average thermodynamic parameters for each descending water, as shown in Table 6. Table 7 then shows the atmospheric partial pressure of CO_2 at the breakpoints in the production curve, and the corresponding total-CO_2 content of each of the descending waters at three saturations, 50, 100, and 200 %.

The total absorption is then

$$Q_i = 0.179\, V_i \sum_{j=1}^{3} \int_0^{T_j} \Delta C_{ij}(t)\, dt,$$

where the numerical factor is (ppm/mole) (m^3/sv-year), i indexes the water masses and j the segments of the production curve, and V_i is the annual production of each water mass. Making use of Table 3, we see that $\Delta C(t) = t\, C_s/T$ for the linear period II, and the integral is $(1/2) C_s T$. During the exponential periods I and II, $\Delta C(t) = C_2 (e^{kt} - 1)$ and the integral is $C_2 (e^{kT} - 1 - kT)/k$.

Absorption values are shown in the lower half of Table 7 and summed at the right, for a total uptake of 5.73 ppm at saturation. Such evidence as is available (Keeling *et al.*, 1965; Brewer, 1978; Chen, Millero, 1979) suggests that the descending waters are consistently undersaturated with CO_2 when they leave the surface (although biological activity may supersaturate them at depth). Curiously, water removes more CO_2 from the atmosphere if it descends consistently undersaturated than if it is supersaturated (because the change in total CO_2 with time is greater for undersaturation). For the sake of argument we will use the saturated value.

In any case, the descending waters carry off nearly half as much CO_2 as the purely diffusive absorption.

Chen and Millero (1979) examine a Geosecs station near 60° in the Southern Ocean, and find a linear increase in anthropogenic CO_2 with depth. Their increase is 0.045 (±0.015) M/T over 700 m, and tracks a similar gradient in the calculated partial pressure, which drops from 300 μatm at the surface to 230 at 700 m. They also follow the minimum salinity layer up the Atlantic (AAI) and the minimum-potential-temperature layer (AAB-NAD), finding enhanced CO_2 at both ends of the Atlantic. Such interpretations require that the carbocline be subtracted out of the data, using the total alkalinity change to correct for $CaCO_3$ from test dissolution and the apparent oxygen utilization to correct for oxidation

Table 7

Total CO_2 content of, and uptake by, descending water masses at various CO_2-saturation percentages S, using the data of Table 6. Although C is calculated to 6 figures to retain 3 "significant" figures in ΔC, it is difficult to measure C to ±0.001, and the calculated increments cannot reliably be detected in historical data.

Year		1858	1917	1940	1979
P	S	292.46	299.27	306.72	337.27
C_{NAD}	50	2.05209	2.05698	2.06218	2.08194
	100	2.18563	2.18954	2.19369	2.20935
	200	2.29016	2.29322	2.29647	2.30883
C_{AAI}	50	2.02286	2.02734	2.03208	2.05008
	100	2.14346	2.14695	2.15066	2.16464
	200	2.23708	2.23985	2.24280	2.25407
C_{AAB}	50	2.08346	2.08793	2.09266	2.11058
	100	2.20317	2.20663	2.21030	2.22413
	200	2.29601	2.29878	2.30172	2.31300
T_j		59	23	39	Q
Q_{NAD}	50	0.3876	0.1605	1.0326	1.5808
	100	0.3101	0.1280	0.8188	1.2570
	200	0.2426	0.1004	0.6466	0.9896
Q_{AAI}	50	1.0162	0.4203	2.6968	4.1332
	100	0.7943	0.3279	2.0962	3.2184
	200	0.6306	0.2612	1.6891	2.5809
Q_{AAB}	50	0.4005	0.1656	1.0616	1.6277
	100	0.3108	0.1283	0.8199	1.2590
	200	0.2488	0.1032	0.6683	1.0202
Totals	50				7.342
	100				5.734
	200				4.591

of organic carbon. High accuracy cannot be expected after such subtractions, and it is encouraging to find that any signal at all can be seen in the noise.

Brewer (1978), using a slightly different transformation of the same data, finds that the calculated initial P of AAB now at 45°S is 300 ppm, while older AAB at 20°S was equilibrated at 250 ppm (but notes that by 20°S AAB has been influenced by mixing with adjacent water masses).

In any event, the increase in CO_2 in the descending waters seems to be just above the detection limit of present technology, and will be increasingly easy to see in the future as the atmospheric level rises.

SUMMARY AND CONCLUSIONS

Table 8 summarizes the results of the diffusive/descending-water model (henceforth denoted "D^2"), showing that ocean and atmosphere together can account for all the industrial CO_2 production. I thank a sharp-eyed reviewer for a critique of improper boundary conditions: the repair raised absorption from a comfortable 92 % to the almost embarrassing value of 99.6 %, but such agreement is surely fortuitous. For comparison, Broecker *et al.* (1979), after considering a number of more involved models, arrive at 91 ± 7 % for this value. D^2 almost certainly overestimates diffusive uptake, because it ignores vertical advection. It also underestimates absorption by descending waters, which as indicated above, are probably undersaturated at descent.

Table 8
Summary of CO_2 absorption by the ocean.

Sink	Q
75 m surface layer	3.76
Diffusive subsurface	19.11
Descending waters	5.73
Totals	28.60
Atmosphere	44.81
Total accounted for	73.41
Production	73.71
Unaccounted for	0.30

One expects errors of 10 % or more. The initial CO_2-production data, according to Keeling (1973), are good only to ± 13 %. The diffusivity and annual volume of descending waters are equally uncertain, and we have not taken into account the smaller water masses. Nor have we considered terrestrial removal as H_2CO_3 reacts with carbonate and basic igneous rocks. Evidently these errors and omissions nearly cancel.

We must also mention non-industrial inputs of CO_2. The two most important are probably oxidation of soil humus under cultivation (Hutchinson, 1954; Bolin, 1977; Lemon, 1977), and deforestation (Stuiver, 1978; Woodwell *et al.*, 1978; Freyer, 1978; May, 1979). The justification for ignoring these sources (which are distinguishable from fossil-fuel by their isotopic ratios) is that they affect the uptake of industrial CO_2 – the topic of this paper – only indirectly. The initial conditions postulated in D^2 are derived principally by back calculation from recent atmospheric measurements using "known" industrial CO_2 production. There is some evidence for pre-industrial CO_2 levels closer to 270 ppm than to 290 (Stuiver, 1978), with the discrepant 20 ppm attributed to deforestation. To model this uptake, the initial oceanic level of total CO_2 would have to be set slightly lower (cf. the low partial pressure reported by Brewer (1978) and Chen and Millero (1979). The growth of atmospheric CO_2 would need to be changed to reflect the rate of agricultural input, but this is a very poorly known function indeed! The overall effect, with lower initial values in both sea and air, and a different set of boundary conditions for the diffusion equation, and different concentrations in descending waters, would, I suspect, be little different from the present model, and the predictions (which hardly depend upon conditions during the period of deforestation, if as Stuiver suggests, this occured primarily between 1860 and 1930) would be unchanged.

D^2, of course, makes no predictions, since it is a retrospective model only. Its relevance to evaluating future threats is indirect, and it should therefore be read in conjunction with an earlier air-sea equilibrium model ("MM", MacIntyre, 1978 *a*) for future values.

Perhaps the most useful achievement of D^2 is its reasonable mechanistic rationale for the 575 m-deep surface box required by MM. Although MM was tolerant of a 10-year lag between production of CO_2 and its absorption by the ocean, or of a 10-ppm disequilibrium, the published version assumed an implausible annual equilibrium between air and the deep surface box. D^2 shows that this is not a serious constraint, because maintenance of the surface boundary condition requires only equilibrium between the wind-stirred layer and the atmosphere. It is difficult to imagine a future industrial CO_2 output so large that this condition could not be fulfilled.

One of the salient features of MM was its prediction of an atmospheric increase at the upper limit of the estimates of kinetic box models which neglect thermodynamics. This faster rise to 600 ppm by AD 2030 is firmly supported by the results of D^2.

REFERENCES

Alexandersson E. T., 1975. Etch patterns on calcareous sediment grain: petrographic evidence of marine dissolution of carbonate minerals, *Science*, **189,** 47-48.

Anderson N. R., Malahoff A., 1978. *The Fate of Fossil-Fuel CO_2 in the Oceans*, Plenum Press, New York.

Armstrong G., 1974. World coal resources and their future potential, *R. Soc. London Philos. Trans.*, **A 276,** 439-456.

Arrhenius S., 1896. On the influence of carbonic acid in the air upon the temperature of the ground, *Philos. Mag.*, **41,** 237-276.

Augustsson T., Ramanathan V., 1977. A radiative-convective model study of the CO_2-climate problem, *J. Atmos. Sci.*, **34,** 448-451.

Bacastow R., 1976. Modulation of atmospheric CO_2 by the Southern Oscillation, *Nature*, **261,** 116-118.

Bacastow R., Keeling C. D., 1973. Atmospheric carbon dioxide and radiocarbon in the natural carbon cycle. II Changes from AD 1700 to AD 2070 as deduced from a geochemical model, in: *Carbon and the Biosphere*, edited by G. M. Woodwell and E. Pecan, AEC Symposium Series, CONF-720510, 86-135.

Bolin B., 1977. Changes of land biota and their importance for the carbon cycle, *Science*, **196,** 613-615.

Bolin B., Eriksson E., 1959. Changes in the carbon dioxide content of the atmosphere and sea due to fossil-fuel combustion, in: *The Atmosphere and the Sea in Motion, Rossby Memorial Volume*, edited by B. Bolin, Rockefeller Inst. Press, New York, 130-142.

Brewer P. G., 1978. Direct observation of the oceanic CO_2 increase, *Geophys. Res. Lett.*, **5,** 997-1000.

Broecker H. C., 1979. The influence of wind on CO_2-exchange in a wind-wave tunnel, including the effects of monolayers, *J. Mar. Res.*, **36,** 595-610.

Broecker W. S., 1975. Climate change: are we on the brink of a pronounced global warming?, *Science*, **189,** 460-463.

Broecker W. S., Peng W. S., 1974. Gas exchange rates between sea and air, *Tellus*, **26,** 21-35.

Broecker W. S., Takahashi T., Simpson H. J., Peng T. H., 1979. Fate of fossil-fuel carbon dioxide and the global carbon budget, *Science*, **206,** 409-418.

Buch K., 1930. Die Kohlensäurefktoren des Meerwassers, *Rapp. P.-V. CPIEM*, **67,** 51-88.

Callendar G. S., 1938. The artificial production of carbon dioxide and its influence on temperature, *Q. J. R. Meteorol. Soc.*, **64,** 223-237.

Chamberlin T. C., 1897-1899. A group of hypotheses bearing on climatic changes, *J. Geol.*, **4,** 653-683.

Chen G. T., Millero F. J., 1979. Gradual increase of oceanic CO_2, *Nature*, **277,** 205-206.

Colville A. J., 1977. Movement of Antarctic ice fronts measured from satellite imagery, *Polar Rec.*, **18,** 390-394.

Craig H., 1957. The natural distribution of radiocarbon and the exchange time of carbon dioxide between the atmosphere and sea, *Tellus*, **9,** 1-17.

Craig H., 1969. Abyssal carbon and radiocarbon in the Pacific, *J. Geophys. Res.*, **74,** 5491-5506.

Craig H., Weiss R. F., 1970. The Geosecs 1969 intercalibration station, *J. Geophys. Res.*, **75,** 7641-7647.

Fairhall A. W., 1973. Accumulation of fossil CO_2 in the atmosphere and sea, *Nature*, **245,** 20-23.

Freyer H. D., 1978. Preliminary evaluation of past CO_2 increase as derived from ^{13}C measurements in tree rings, in: *Carbon dioxide, climate, and society*, edited by J. Williams, Pergamon Press, Oxford, 69-75.

Gordon A. L., 1971. Oceanography of Antarctic Waters, *AGU Antarct. Res. Ser.*, **15,** 169-203.

Gulliksen S., Nydal R., Lovseth K., 1972. Further calculations on the C-14 exchange between the ocean and the atmosphere, *Proc. 8th International Radiocarbon Dating Conference*, Lower Hutt, New Zealand, Oct. 18-25, 1972, C58-C72.

Houtman Th. J., 1967. Water masses and fronts on the Southern Ocean south of New Zealand, *N. Z. Dep. Sci. Ind. Res. Bull.*, **174.**

Hoyt D. V., 1979. An empirical determination of the heating of the Earth by the CO_2 greenhouse, *Nature*, **282,** 388-390.

Hutchinson G. E., 1954. Chapter 8 in: *The Earth as a Planet*, edited by G. Kuiper, Chicago University Press.

Idso S. B., 1980. The climatological significance of a doubling of the Earth's atmospheric carbon-dioxide content, *Science*, **207,** 1462-1463.

Johannes R. E., Satori M., 1966. Composition and nutritive value of fecal pellets of a marine crustacean, *Limnol. Oceanogr.*, **18,** 191-197.

Keeling C. D., 1973*a*. Industrial production of carbon dioxide from fossil-fuel and limestone, *Tellus*, **25,** 1974-1980.

Keeling C. D., 1973*b*. The carbon-dioxide cycle: reservoir models to depict the exchange of atmospheric CO_2 with the oceans and land plants, in: *Chemistry of the lower atmosphere*, edited by S. Rasool, Plenum, New York, 251-329.

Keeling C. D., Bolin B., 1967. The simultaneous use of chemical tracers in oceanic studies (Part I), *Tellus*, **19,** 566-581.

Keeling C. D., Bolin B., 1968. The simultaneous use of chemical tracers in oceanic studies (Part II), *Tellus*, **20,** 17-54.

Keeling C. D., Rakestraw N. W., Waterman L. S., 1965. Carbon dioxide in surface waters, *J. Geophys. Res.*, **70,** 6087-6097.

Keeling C. D., Bacastow R. B., Bainbridge A. E., Ekdahl C. A., Gunehter P. R., Waterman L. S., Chen J. F. S., Cobley U. T., 1976. Atmospheric carbon dioxide variations at Mauna Loa observatory, *Tellus*, **28,** 538-551.

Ketchum B., 1957. The effects of atomic radiation on oceanography and fisheries, Chapt. 5, *Nat. Acad. Sci. Publ.*, **551,** Washington, DC, 52-59.

Lemon E., 1977. The land's response to more carbon dioxide, in: *The fate of fossil-fuel CO_2 in the oceans*, edited by N. R. Anderson and A. Malahoff, Plenum Press, New York, 97-130.

Lyman J., 1957. Buffer mechanism of sea water, *Ph. D. Thesis*, Univ. of California, Los Angeles, 196 p.

Machta L., 1972. The role of the oceans and biosphere in the CO_2 cycle, in: *The changing chemistry of the oceans*, edited by D. Dyrsen and D. Jagnar, Almqvist and Wikset, Stockholm, 121-160.

MacIntyre F., 1978*a*. Toward a minimal model of the world CO_2 system. I. Carbonate-alkalinity version, *Thalassia Jugosl.*, **14,** 63-94.

MacIntyre F., 1978*b*. On the temperature coefficient of P_{CO_2} in seawater, *Climatic Change*, **1,** 349-354.

MacIntyre F., 1980. The air-sea partition functions for CO_2, submitted to *Mar. Chem.*

Manabe S., Wetherald R. T., 1975. The effects of doubling the CO_2 concentration on the climate of a general circulation model, *J. Atmos. Sci.*, **32,** 3-15.

May R. M., 1979. Nutrient retention in tropical rain forests, *Nature*, **282,** 13.

Menzel D. W., 1974. Primary productivity, dissolved and particulate organic matter and the sites of oxidation of organic matter, Chapt. 18, in: *The Sea*, edited by E. D. Goldberg, Wiley-Interscience, New York, Vol. 5, 615.

Mercer J. H., 1978. West Antarctic ice sheet and CO_2 greenhouse effects, a threat of disaster, *Nature*, **271,** 321-325.

Millero F. J., 1979. The thermodynamics of the carbonate system in seawater, *Geochim. Cosmochim. Acta*, **43,** 1651-1661.

Munk W. H., 1966. Abyssal recipes, *Deep-Sea Res.*, **13,** 707-730.

Newell R. E., Dopplick T. G., 1979. Questions concerning the possible influence of anthropogenic CO_2 on atmospheric temperature, *J. Appl. Meteorol.*, **18,** 822-825.

Nydal R., 1968. Further investigation on the transfer of radiocarbon in nature, *J. Geophys. Res.*, **73,** 3617-3635.

Oeschger H., Siegenthaler U., Schotterer U., Guglemann A., 1975. A box diffusion model to study the CO_2 exchange in nature, *Tellus*, **27,** 168-192.

Packard T. T., 1971. The measurement of respiratory electron transport activity in marine phytoplankton, *Limnol. Oceanogr.*, **16,** 60-70.

Plass G. M., 1956. The CO_2 theory of climatic change, *Tellus*, **8,** 149-154.

Rafter T. A., O'Brien B. J., 1972. ^{14}C measurements in the atmosphere and in the South Pacific Ocean. A recalculation of the exchange rate between the atmosphere and the ocean, in: *Proc. 8th Inter. Conf. on Radiocarbon Dating*, Wellington, New Zealand, 241-266.

Reid J. L., 1973. Northwest Pacific Ocean waters in winter, *The Johns Hopkins Oceanographic Studies*, **5,** 96 p.

Revelle R., Suess H. E., 1957. Carbon dioxide exchange between atmosphere and ocean and the question of an increase of atmospheric CO_2 during the past 2 decades, *Tellus*, **9,** 18-27.

Riley G. A., 1951. Oxygen, phosphate, and nitrate in the Atlantic Ocean, *Bingham Oceanogr. Colloq. Bull.*, **13,** 1.

Rotty R. M., 1977. Global carbon-dioxide production from fossil-fuels and cement, AD 1950-AD 2000, in: *The fate of fossil-fuel CO_2 in the oceans*, edited by N. R. Anderson and A. Malahoff, Plenum Press, New York, 167-182.

Schneider J. H., 1975. On the carbon-dioxide-climate confusion, *J. Atmos. Sci.*, **32,** 2060-2066.

Stuiver M., 1978. Atmospheric carbon dioxide and carbon-reservoir changes, *Science*, **199,** 253-258.

Suess H. E., 1970. Transfer of carbon-14 and tritium from the atmosphere to the ocean, *J. Geophys. Res.*, **75,** 2363-2364.

Thomas R. H., Sanderson T. J. O., Rose K. E., 1979. Effect of climate warming on the West Antarctic ice sheet, *Nature*, **277,** 355-358.

Tyndall J., 1961. On the absorption and radiation of heat by gases and vapours, and on the physical connection of radiation, absorption, and conduction, *Philos. Mag.*, **22** (Ser. 4), 169-194; 273-285.

van Slyke D. D., 1922. The measurement of buffer values and the relationship of buffer value to the dissociation constant of the buffer and the concentration and reaction of the buffer solution, *J. Biol. Chem.*, **52,** 525-570.

Vinogradov M. Ye., 1961. Food sources of the deep-water fauna. Speed of decomposition of dead Pteropoda, *Am. Geophys. Union*, **136/141,** 39-42, Dokl. Akad. Nauk. SSSR Okeanol.

Weiss R. F., 1974. Carbon dioxide in water and seawater: the solubility of a non-ideal gas, *Mar. Chem.*, **2,** 203-215.

Woodwell G. M., Whitakker R. H., Runers W. A., Lukens G. E., Delwick C. C., Botkin D. B., 1978. The biota and the world carbon budget, *Science*, **199,** 141-146.

Wyrtki K., 1962. The oxygen minimum in relation to ocean circulation, *Deep-Sea Res.*, **9,** 11-23.

Zimen K. E., Altenheim F. K., 1973. The future burden of industrial CO_2 on the atmosphere and the oceans, *Naturwissenschaften*, **60,** 198-199.